



ALMA MATER STUDIORUM  
UNIVERSITÀ DI BOLOGNA

## ARCHIVIO ISTITUZIONALE DELLA RICERCA

### Alma Mater Studiorum Università di Bologna Archivio istituzionale della ricerca

Ecological regime shift preserved in the Anthropocene stratigraphic record

This is the final peer-reviewed author's accepted manuscript (postprint) of the following publication:

*Published Version:*

Tomasovych A., Albano P.G., Fuksi T., Gallmetzer I., Haselmair A., Kowalewski M., et al. (2020). Ecological regime shift preserved in the Anthropocene stratigraphic record. PROCEEDINGS - ROYAL SOCIETY. BIOLOGICAL SCIENCES, 287(1929), 1-9 [10.1098/rspb.2020.0695].

*Availability:*

This version is available at: <https://hdl.handle.net/11585/766621> since: 2024-05-22

*Published:*

DOI: <http://doi.org/10.1098/rspb.2020.0695>

*Terms of use:*

Some rights reserved. The terms and conditions for the reuse of this version of the manuscript are specified in the publishing policy. For all terms of use and more information see the publisher's website.

This item was downloaded from IRIS Università di Bologna (<https://cris.unibo.it/>).  
When citing, please refer to the published version.

(Article begins on next page)

# PROCEEDINGS OF THE ROYAL SOCIETY B

BIOLOGICAL SCIENCES

## Ecological regime shift preserved in the Anthropocene stratigraphic record

Journal:	<i>Proceedings B</i>
Manuscript ID	RSPB-2020-0695
Article Type:	Research
Date Submitted by the Author:	27-Mar-2020
Complete List of Authors:	Tomasovych, Adam; Slovak Academy of Sciences, Earth Science Institute Albano, Paolo; University of Vienna, Department of Palaeontology Fuksi, Tomas; Slovak Academy of Sciences, Earth Science Institute Gallmetzer, Ivo; University of Vienna, Department of Palaeontology Haselmair, Alexandra; University of Vienna, Department of Palaeontology Kowalewski, Michal; University of Florida, Florida Museum of Natural History Nawrot, Rafał; University of Vienna, Department of Palaeontology Nerlovic, Vedrana; University of Split, Department of Marine Sciences Scarponi, Daniele; University of Bologna, Dipartimento di Scienze Biologiche, Geologiche e Ambientali Zuschin, Martin; University of Vienna, Department of Palaeontology
Subject:	Palaeontology < BIOLOGY, Ecology < BIOLOGY
Keywords:	conservation paleobiology, stratigraphic paleobiology, time averaging, regime shift, stasis, Adriatic Sea
Proceedings B category:	Palaeobiology

SCHOLARONE™  
Manuscripts

**Author-supplied statements**

Relevant information will appear here if provided.

***Ethics***

*Does your article include research that required ethical approval or permits?:*

This article does not present research with ethical considerations

*Statement (if applicable):*

CUST\_IF\_YES\_ETHICS :No data available.

***Data***

*It is a condition of publication that data, code and materials supporting your paper are made publicly available. Does your paper present new data?:*

Yes

*Statement (if applicable):*

All size and compositional data are attached in an excel file in the Supplement, plus source codes in R language

***Conflict of interest***

I/We declare we have no competing interests

*Statement (if applicable):*

CUST\_STATE\_CONFLICT :No data available.

***Authors' contributions***

This paper has multiple authors and our individual contributions were as below

*Statement (if applicable):*

A.T. and M.Z. designed the research, P.A., T.F., I.G., A.H., M.K., R.N., V.N. and D.S. collected the data, A.T. compiled and analyzed the data, and all authors discussed the results and contributed to the writing of the manuscript.

1 Title: Ecological regime shift preserved in the Anthropocene stratigraphic record

2

3 Running Head: Regime shift in the stratigraphic record

4

5 Authors: Adam Tomašových<sup>1,2</sup>, Paolo G. Albano<sup>2</sup>, Tomáš Fuksi<sup>1</sup>, Ivo Gallmetzer<sup>2</sup>, Alex  
6 Haselmair<sup>2</sup>, Michał Kowalewski<sup>3</sup>, Rafał Nawrot<sup>2</sup>, Vedrana Nerlović<sup>4</sup>, Daniele Scarponi<sup>5</sup>,  
7 Martin Zuschin<sup>2</sup>

8

9 Affiliations: <sup>1</sup>Earth Science Institute, Slovak Academy of Sciences, Dúbravská cesta 9, 84005  
10 Bratislava, Slovakia

11 <sup>2</sup>University of Vienna, Department of Palaeontology, Althanstrasse 14, 1090 Vienna

12 <sup>3</sup>Florida Museum of Natural History, University of Florida, 1659 Museum Road, Gainesville,  
13 FL 32611, USA

14 <sup>4</sup>Department of Marine Studies, University of Split, Ruđera Boškovića 37, 21000 Split,  
15 Croatia

16 <sup>5</sup>Department of Biological, Geological and Environmental Sciences, University of Bologna,  
17 Piazza di Porta San Donato 1, I-40126 Bologna, Italy

18

19

20 Corresponding author: Adam Tomašových, Earth Science, Slovak Academy of Sciences,  
21 Dúbravská cesta 9, 84005 Bratislava, Slovakia. Tel: 00421-904-852145, Email:  
22 geoltoma@savba.sk

23

24 Keywords: conservation paleobiology, stratigraphic paleobiology, stasis, regime shift, time

25 averaging, northern Adriatic Sea

## 26 **SUMMARY**

27 Paleocological data are unique historical archives that extend back far beyond the last several  
28 decades of ecological observations. However, the fossil record of continental shelves has been  
29 perceived as too coarse and incomplete to detect processes occurring at decadal scales  
30 relevant to ecology and conservation. Here we show that the youngest (Anthropocene) fossil  
31 record on a continental shelf of the Adriatic Sea provides decadal-scale temporal resolution  
32 that is adequate for documenting an abrupt ecological shift affecting benthic communities  
33 during the 20<sup>th</sup> century. The magnitude and the duration of the 20<sup>th</sup> century shift in body size  
34 of a dominant bivalve species (*Corbula gibba*) is unprecedented given that this species was  
35 consistently small throughout the Holocene in the whole northern Adriatic Sea. The size shift  
36 coincided with compositional change of the benthic community, with the median per-  
37 assemblage abundance of *C. gibba* increasing from ~25% to ~70% in the late 20<sup>th</sup> century,  
38 and occurred at sites that experienced at least one hypoxic event per decade in the 20<sup>th</sup>  
39 century. This regime shift, which coincided with mass mortality of competitors and predators  
40 associated with higher frequency of seasonal hypoxic events, may reflect ecological release.  
41 The observed body size shift is coupled with a decline in the depth and rate of bioturbational  
42 mixing. This decline in burrowing benthic organisms resulted in the improved stratigraphic  
43 resolution of fossil assemblages, making it possible to detect sub-centennial ecological  
44 changes in the stratigraphic record on continental shelves.

45

## 46 **Significance statement**

47 The stratigraphic records of deep-time ecosystem perturbations are not equivalent to  
48 chronological records of Anthropocene ecological collapses because these two types of  
49 archives differ in stratigraphic completeness and time averaging. Although conservation  
50 paleobiology approaches identify past baselines and detect differences between the Holocene

51 and present-day communities, it remains unclear if Holocene-Anthropocene stratigraphic  
52 records can inform us about rates of ecological change. We show that the 20<sup>th</sup> century  
53 stratigraphic record of molluscan assemblages in cores in the Adriatic Sea uniquely detects an  
54 abrupt, decadal-scale regime shift in size structure and species composition of molluscan  
55 assemblages that has no precedents in the Holocene record. This decadal-scale resolution was  
56 made possible by intensification of hypoxia that not only led to a competitive and predatory  
57 release but also reduced bioturbation and thus enhanced temporal resolution of the  
58 stratigraphic record. We highlight a dichotomy in the resolution of the fossil record between  
59 background regimes with low incidence of major ecosystem perturbations with highly time-  
60 averaged fossil assemblages and disturbance or extinction regimes such as Anthropocene  
61 when limited bioturbation suppresses time averaging.

62

## 64 **1. Introduction**

65 Although high-resolution time series based on monitoring of living assemblages can directly  
66 detect the dynamics of marine ecosystem responses to stressors (1-5), their duration is  
67 typically decadal (6-7). Therefore, they might not detect former baseline states or discriminate  
68 short-term fluctuations from sustained regime shifts. In contrast, surface and subsurface  
69 stratigraphic records that capture longer durations led to unique discoveries of ecosystem  
70 shifts driven by pollution, eutrophication or overfishing that occurred over the past centuries  
71 or millennia (8-12). These shifts can be comparable in magnitude to ecological crises that  
72 occurred during the mass extinctions when deoxygenation and warming also significantly  
73 contributed to the demise of ecosystems (13-15). However, determining whether the  
74 ecological changes were gradual or abrupt on the basis of the stratigraphic record is hindered  
75 by hiatuses (induced by erosion and non-deposition) and by time averaging (mixing of non-  
76 contemporaneous generations) (16-17), unless bioturbation is limited and erosion is rare or  
77 episodic as in lacustrine or anoxic environments (18-20). As a result, benthic fossil  
78 assemblages from continental shelves – settings that provide the bulk of the deep-time  
79 paleontological data on ecological dynamics – are incomplete and temporally mixed over  $10^3$ -  
80  $10^4$ -year time scales (21-22). On one hand, both the hiatuses and the time averaging of  
81 bioturbated sediments depress the magnitude of ecological change *over a given timespan* (23-  
82 25). On the other hand, hiatuses can generate apparently abrupt shifts in the magnitude of  
83 ecological change *over a given stratigraphic distance* even in the absence of truly abrupt  
84 regime shifts, confounding assessments of ecological turnover on the basis of stratigraphic  
85 records (24-26).

86 The Holocene cores recording anthropogenic impacts provide a unique testing  
87 opportunity to assess whether the response of marine ecosystems exposed to disturbance can  
88 be resolved from stratigraphic records. Here, absolute dating of shells embedded in sediment

89 cores allows us to directly compare *chronological* (i.e., ages of fossils in time series do not  
90 depend on their stratigraphic position, here partitioned into 5-year age cohorts) and  
91 *stratigraphic* records (i.e., ages of fossils refer to the mean age of a sedimentary layer in  
92 which they are embedded). We test whether the responses of benthic communities to  
93 eutrophication and hypoxic events that intensified in the Adriatic Sea (figure 1A) during the  
94 late 20<sup>th</sup> century left high-resolution signatures in the Anthropocene stratigraphic record  
95 (informally denoting here the 20<sup>th</sup> and 21<sup>st</sup> centuries) (1) by assessing chronologic and  
96 stratigraphic changes in mean and maximum body size of an opportunistic and hypoxia-  
97 tolerant bivalve (*Corbula gibba*) in sediment cores and (2) by comparing molluscan species  
98 composition between Holocene and Anthropocene assemblages. We suggest that bioturbated  
99 sediment cores can generate high-resolution windows into ecological dynamics induced by  
100 disturbances such as oxygen depletion that subsequently limit sediment mixing.

101 We focus on body size because this attribute tracks ecosystem changes during natural  
102 (27) and anthropogenic disturbances of ecosystems (28-29) and also predicts present-day  
103 extinction threat of marine molluscs (30). We combine body size estimates based on valve  
104 length measurements of 20,774 specimens of *C. gibba* collected with cores split into ~5-10  
105 cm-thick increments and 14 surface death assemblages with formerly-published estimates of  
106 time averaging based on radiocarbon-calibrated amino acid racemization (figure 2, see  
107 electronic supplementary material, ESM). First, we identify the number and timing of abrupt  
108 shifts in the mean and the 95th percentile log-length in chronological and stratigraphic records  
109 with the threshold regression (31). Second, we test whether models that allow for abrupt shifts  
110 in size have higher support than models with stasis or trends (32) and assess their sensitivity  
111 to time averaging. Third, we assess whether these shifts covary with independent estimates of  
112 changes in bottom-water oxygen concentrations and whether they are associated with  
113 compositional changes in molluscan communities.

114

115 **2. Methods**

116 **(a) Sediment cores, dating, and time averaging.** Death assemblages of *Corbula gibba* were  
117 collected in Holocene cores and with Van Veen grabs in the northern Adriatic Sea. First, 1.5  
118 m-long cores were collected at eight sites at water depths between 10 and 44 m (two sites at  
119 Po prodelta, two sites at Isonzo prodelta, two sites off Piran, and one site at Venice and  
120 Brijuni). Second, one 26 m-long Holocene section of S10 core was collected at the Po Plain  
121 (33). Third, Van Veen grabs (~upper 10 cm) were collected at 14 sites at Po prodelta (2 sites),  
122 in the Gulf of Venice (2 sites), off Rovinj (2 sites), and in the Bay of Panzano (Isonzo  
123 prodelta) in the northern Gulf of Trieste (8 sites) (figure S1). Estimates of increment ages,  
124 sedimentation rates, and time averaging of all cores based on ages (AAR calibrated by  $^{14}\text{C}$ ) of  
125 four targeted molluscan species were published in our previous studies (34-40). Time  
126 averaging corresponds to an inter-quartile age range in years (IQR) in ~10-30 cm-thick units  
127 on the basis of AAR calibrated by  $^{14}\text{C}$  in four molluscan species (34-40). Net sedimentation  
128 rate was ~0.3 cm/y during the transgressive phase (TST) and 1-2 cm/y during the highstand  
129 phase (HST) at Po prodelta, 0.2-0.4 cm/y during the HST phase at Isonzo prodelta, and ~0.01  
130 cm/y during the TST and HST phases off Istria and in the Gulf of Venice (36-40). The  
131 uppermost HST increments (corresponding to 20<sup>th</sup> century sediments) do not show any signs  
132 of increased or decreased sedimentation rate (36). The differences in net sedimentation rates  
133 translate to differences in IQR. First, highly time-averaged assemblages (IQR = ~1,000-2,000  
134 years) occur in TST (S10, Venice, Piran, Brijuni) and HST increments (Venice, Piran,  
135 Brijuni), including mixtures of highstand and Anthropocene shells in topcore and surface  
136 assemblages at Rovinj, Venice, Piran, and Brijuni. Second, weakly time-averaged  
137 assemblages (IQR = ~10-200 years) occur in HST increments and Anthropocene increments  
138 at Po and Isonzo prodeltas. The cores with weakly time-averaged assemblages show a

139 significant upcore decline in IQR in the 20<sup>th</sup> century sediments at Po (from decadal to yearly  
140 IQR) and Isonzo prodeltas (from centennial to decadal IQR, 36). This stratigraphic upcore  
141 decline in IQR is driven by a decrease in the bioturbation depth and rate rather than by an  
142 increase in sedimentation rate (36).

143  
144 **(b) Size data.** We measured shell size with the length of right valves in 20,774 specimens of  
145 *C. gibba*. *Chronological* analyses in body size are based on lengths of specimens from two Po  
146 cores that were directly dated (36) and were partitioned into 5-year age cohorts (table S1-S2,  
147 252 dated specimens at Po 3 and 243 dated specimens at Po 4, sample sizes of cohorts that  
148 lived in the 19<sup>th</sup> and 20<sup>th</sup> century in other cores are low). *Stratigraphic* analyses of size  
149 distributions are performed (1) at the scale of 5-10 cm-thick increments and (2) by pooling  
150 these increments to 10-30 cm-thick units characterized by homogeneous sedimentologic  
151 composition (72 samples in total) and at two spatial scales, including (1) pooling closely-  
152 located sites to three localities (Po, Isonzo, Piran), and (2) at the scale of eight individual sites  
153 (table S1, S3-S4). Size data are available in the electronic supplementary material.

154  
155 **(c) Multivariate size analyses.** We assess whether size structure did undergo a shift in the  
156 20<sup>th</sup> century to a new state, using principal coordinate analysis, with the Frechet distances  
157 between 10-30 cm-thick increments, based on proportional abundances of 1 mm cohorts and  
158 (figure S2A-B). The multivariate analyses are thus based on 72 samples (in analyses based on  
159 all shells based on 20,774 specimens) and 66 samples (in analyses based on shells with  
160 periostracum based on 13,985 specimens). They are assigned to four stratigraphic units,  
161 including (1) TST (between 10-7 kyr ago), (2) HST (here, referring to increments deposited  
162 prior to the late 20<sup>th</sup> century), (3) topcore samples with a strongly time-averaged mixture of  
163 the HST and the 20<sup>th</sup> century sediments deposited under <0.01 cm/y (HST-Anthropocene),

164 and (4) the topcore samples at Po and Isonzo prodeltas deposited under  $>0.2$  cm/y and  
165 corresponding to the late 20<sup>th</sup> century (Anthropocene). We use analogue matching analyses to  
166 assess whether Anthropocene assemblages extend beyond the variation defined by all  
167 Holocene (TST and HST) assemblages in terms of Frechet distances between the Holocene  
168 centroid and individual Anthropocene assemblages (41-44) and evaluate differences in size  
169 structure between four stratigraphic units with permutational multivariate analysis of variance  
170 (PERMANOVA, 45). To untangle these cohorts, we scored all shells in Van Veen grab  
171 samples on the basis of periostracum preservation. Periostracum is usually not preserved on  
172 shells older than 19<sup>th</sup>-20<sup>th</sup> century (figure S3).

173  
174 **(d) Detection of regime shifts and sensitivity to time averaging.** We compare chronological  
175 and stratigraphic records in (i) the mean and (ii) the 95% percentile log-length. The mean  
176 length captures the central tendency across the whole size range of death assemblages,  
177 including juvenile specimens, whereas the 95% percentile length is informative about the size  
178 structure of adult individuals. We use three approaches to detect the regime shifts (i.e., a  
179 large, abrupt, and persistent shift in ecosystem structure), here approximated by shift in the  
180 size structure of one of the most abundant molluscan species). First, a threshold regression  
181 identifies abrupt shifts and their location in chronological or stratigraphic time series. We use  
182 an F statistic that evaluates whether the model with one shift explains significantly more than  
183 the model with just an intercept (31) and the adjusted  $R^2$  to compare the threshold model with  
184 a simple linear model. Second, we fit chronological or stratigraphic time series of size to  
185 likelihood models of the unbiased random walk, stasis, and directional trends (32, 46-47). In  
186 total, the likelihood models discriminate among four modes (stasis, strict stasis, random walk,  
187 and directional models) and allow for one abrupt shift between them (nine models in total, we  
188 set the minimum segment length to 7 samples). The stasis model is considered as

189 uncorrelated, normally-distributed variation in size (either in the mean or in the 95th  
190 percentile log-length), with temporal variance  $\omega$  around a stable long-term mean  $\theta$  (48). Size  
191 is expected to converge immediately to  $\theta$  from any precursor (ancestral) value. The variance  
192  $\omega$  is zero under the so-called strict stasis. Directional shift in body size models a size change  
193 for each time step on the basis of a normal distribution of size changes, with mean size change  
194  $\mu_s$  and a variance of size changes  $\delta_s^2$ . A random walk is a special case of the directional model  
195 in which  $\mu_s$  is equal to zero and the distribution of size changes is also normal, with variance  
196 also equal to  $\delta_s^2$ . The punctuation model refers to one abrupt shift separated by two segments  
197 of stasis with  $\theta_1$  and  $\theta_2$  and a single  $\omega$ , and is thus conceptually most comparable to the  
198 definition of the regime shift. We estimate the number and timing of shifts with threshold  
199 regression (figure S4-S6) and the support for nine models in (1) whole cores and (2) core  
200 subsets with HST and Anthropocene increments for both chronologic and stratigraphic series  
201 (table S3-S4). Third, we correlate the model support and  $\omega$  with time averaging (IQR) for (1)  
202 the HST core subsets and (2) the core subsets with HST and Anthropocene increments.

203

204 **(e) Covariates of size shifts.** We assess the response of the mean and 95<sup>th</sup> percentile log-  
205 length to a hypothesized driver - yearly frequency of seasonal hypoxia (dissolved oxygen  
206 concentrations  $< 2$  ml/L) on the basis of instrumental measurements performed between 1970-  
207 2010 - with the threshold regression and generalized additive models. Second, we compare  
208 the taxonomic composition of molluscan assemblages with TST and HST assemblages on one  
209 hand (deposited prior to the 20<sup>th</sup> century or during the earliest 20<sup>th</sup> century, 95 assemblages  
210 from the same cores used in analyses of shell size) with 54 Anthropocene death assemblages  
211 (late 20<sup>th</sup> century) and 223 Anthropocene living assemblages collected since 1980s on the  
212 other hand (Van Veen grab samples compiled from published sources). The Anthropocene  
213 data are based on multiple studies by various authors of soft-bottom habitats in the Po

214 prodelta and in the Gulf of Trieste between 10-30 m water depth (with sample size exceeding  
215 30) and are thus standardized to genus level. The compositions of Anthropocene living  
216 assemblages are not affected by mixing and thus help constraining the compositional state of  
217 the latest 20<sup>th</sup> century communities. Compositional differences are analyzed with principal  
218 coordinate analysis, PERMANOVA (Bray-Curtis distances based on square-root transformed  
219 proportional abundances of genera), and with the analogue matching by evaluating whether  
220 Anthropocene assemblages extend beyond the variation defined by the Holocene assemblages  
221 (using Bray-Curtis distances between the Holocene centroid and individual Anthropocene  
222 assemblages, 41-45).

223  
224 **(f) Effects of time averaging on regime shifts in simulations.** We investigate the effect of  
225 time averaging on the detection of the regime shift over a broad range of values, from 1 year  
226 up to 1,000 years in simulations. This range reflects the IQR values observed in the Adriatic  
227 Sea: time averaging varies by two orders of magnitude between the Po prodelta with decadal  
228 IQR, the Isonzo prodelta with centennial IQR, and sites off Istria with millennial IQR. We  
229 simulate the effects of time averaging (1) on the timing and the abruptness of shifts and (2) on  
230 the estimate of  $\omega$  with two scenarios. In a first scenario, we assess the sensitivity of  $\omega$  in a  
231 stasis model with  $\theta_1 = 1$  in a Holocene-scale simulation with 10,000 years, varying true  $\omega$   
232 between 0.01 and 0.2 (values comparable to empirical estimates). In a second scenario,  
233 tailored to the past 200 years to capture sedimentation conditions at Po and Isonzo prodeltas,  
234 the abrupt increase in size from  $\theta_1 = 1$  (2.7 mm) to  $\theta_2 = 2$  (7.4 mm) occurs in 1950 and the  
235 true  $\omega$  of non-averaged time series is set to 0.01. In this Anthropocene simulation, we assess  
236 what eco-evolutionary size models are best supported as time averaging increases. In both  
237 scenarios, we sample 50 individuals in each of the thirty increments (comparable to the  
238 number of increments and sample sizes in 1.5 m-long cores), and fit time-averaged time series

239 with the same methods as empirical time series. We repeat simulations 1,000 times, estimate  
240 means of  $\omega$  in Holocene-scale simulations, and compute model-specific Akaike weights in  
241 Anthropocene simulations, with 95% confidence intervals.

242

### 243 **3. Results**

#### 244 *(a) Size shift in the northern Adriatic Sea*

245 The size structure of *C. gibba* in Anthropocene assemblages (figure 1B) does not overlap with  
246 TST (10-7 kyr ago) and HST (~7 kyr ago up to the 19<sup>th</sup> century) assemblages in principal  
247 coordinate analysis (figure 1B, table S5-S6), and 50% of Anthropocene assemblages are  
248 farther from the Holocene centroid in terms of the Frechet distances than 97.5% of Holocene  
249 assemblages (figure 2A). TST and HST increments do not differ in size structure and are both  
250 characterized by right-skewed, thin-tailed distributions dominated by individuals < 5 mm  
251 (black histograms in figure 1A). Anthropocene assemblages (white histograms in figure 1A)  
252 from high-sedimentation sites (>0.2 cm/y) with centennial to decadal IQR at the Po and  
253 Isonzo prodeltas are characterized by bimodal distributions with abundant large individuals (>  
254 10 mm). Low-sedimentation sites with millennial IQR generated by mixing of Anthropocene  
255 and HST assemblages in top-core increments are characterized by heavy-tailed distributions,  
256 with individuals > 5 mm being moderately frequent (figure 1A). The shift between the TST  
257 and HST assemblages on one hand and Anthropocene assemblages on the other hand is driven  
258 by the appearance of individuals > 10 mm. The mean and the 95<sup>th</sup> percentile log-length of *C.*  
259 *gibba* in death assemblages correlate positively with the 1970-2010 measurements of yearly  
260 frequency of seasonal hypoxia at 16 sites (Spearman  $r = 0.91$ ,  $p = 0.005$ ) and the 95<sup>th</sup>  
261 percentile log-length (Spearman  $r = 0.82$ ,  $p < 0.0001$ ). The 95<sup>th</sup> percentile log-length increases  
262 abruptly at 10% probability of yearly hypoxia (figure 2B), suggesting that the switch from the  
263 right-skewed to bimodal state occurs at low frequency of hypoxia.

264

265 ***(b) Compositional shift in the northern Adriatic Sea***

266 The size shift coincides with a shift in the molluscan composition. The Bray-Curtis distances  
267 show that 82% of Anthropocene living assemblages are further from the Holocene centroid  
268 than 97.5% of individual Holocene assemblages (figure 2B). The Holocene abundance  
269 increases from ~20-30% (95% confidence intervals on the median value) in TST and HST  
270 increments to 50-60% in time-averaged death assemblages and to 63-75% in Anthropocene  
271 non-averaged living assemblages (figure 2C). The increase in abundance of *C. gibba* is  
272 compensated by the decline in abundance of commensals, predators and scavengers (figure  
273 S7). Principal coordinate analyses and PERMANOVA show that the overlap between  
274 Anthropocene living and death assemblages on one hand and Holocene assemblages on the  
275 other hand is negligible (figure 2E, table S5).

276

277 ***(c) Chronological and stratigraphic record of size shifts***

278 Threshold regressions and model fitting show that chronological records in size at Po are best  
279 explained by an abrupt punctuational increase in the mean log-length (from  $\theta_1 = 1.07$  to  $\theta_2 =$   
280  $1.53$ , with  $\omega = 0.007$ ) and in the 95<sup>th</sup> percentile log-length (from  $\theta_1 = 1.6$  to  $\theta_2 = 2.3$ , with  $\omega =$   
281  $0.022$ ) that occurred within a single decade at ~1950 (figure 3A, 4A). This shift separates  
282 populations exhibiting stasis prior to (right-skewed distributions) and after 1950 (bimodal  
283 distributions). Stratigraphic records at sites with high sedimentation ( $> 0.2$  cm/y) at Po and  
284 Isonzo also support a single abrupt shift both in the mean and the 95<sup>th</sup> percentile log-length (in  
285 the mid-20<sup>th</sup> century at 80-110 cm at Po and in the late 19<sup>th</sup> century at 30-35 cm at Isonzo,  
286 figure 3B, 4B). These shifts are best explained by the punctuation between two stasis  
287 segments or by the shift from stasis to random walk (figure 3B), and thus capture similar  
288 dynamics as the chronological records. In contrast, stratigraphic records at sites with slow

289 sedimentation ( $\sim 0.01$  cm/y) either detect a size decline between the TST and HST units or do  
290 not show any shifts, and estimates of  $\omega$  are smaller than at Po and Isonzo (figure 4C).  
291 Although the signature of the size increase in the 20<sup>th</sup> century is lost at these sites, TST and  
292 HST assemblages are consistently dominated by small-size individuals whereas the top-core  
293 mixtures of highstand and Anthropocene shells averaged to millennia are heavy-tailed and  
294 thus still detect the signature of the 20<sup>th</sup> century size increase (figure 1B). These heavy-tailed  
295 assemblages become bimodal when old shells without the surficial periostracum layer are  
296 excluded (figure S2-S3). Therefore, body size shifts during the Holocene until the 20<sup>th</sup> century  
297 are of smaller magnitude than the size increase observed in the 20<sup>th</sup> century.

298         Although the Po and Isonzo records with the upcore transition from centennial to  
299 decadal averaging in the 20<sup>th</sup> century deposits capture the abrupt increase in size relatively  
300 well, size changes within HST increments at sites with millennial averaging are very muted  
301 and support a single stasis model (figure 4A-B). This difference in the stratigraphic  
302 expression of size pattern is confirmed by simulations of abrupt size-increase in 1950, which  
303 predict that the punctuation is preserved when the magnitude of time averaging does not  
304 exceed  $\sim 20$ -50 years (figure 4D-E). The variance ( $\omega$ ) in the mean and in the 95<sup>th</sup> percentile  
305 log-length declines by two orders of magnitude with time averaging increasing from decadal  
306 to millennial values, both in the empirical and simulated stratigraphic records (figure 4C, FF).  
307 This effect pulls the size trajectory in the stratigraphic record towards stronger stasis and  
308 towards very small  $\omega$  at sites with slow sedimentation. The pull by time averaging is avoided  
309 at Po and Isonzo because punctuations at these sites coincide with the upcore decline in time  
310 averaging from 30 to  $\sim 15$  years at Po and from 75 to  $\sim 10$ -20 years at Isonzo (figure 2). The  
311 stratigraphic records at the Po and Isonzo prodeltas thus distinctly preserve the 20<sup>th</sup> century  
312 shift (under high or moderate sediment accumulation rates) because IQRs of the late 20<sup>th</sup>  
313 century assemblages are low. Under higher depth and rate of bioturbation that characterized

314 these environments prior to 1950s, multi-decadal time averaging strongly mutes the  
315 stratigraphic signal in size patterns even under relatively high sedimentation rates (figure 4D-  
316 E).

317

#### 318 **4. Discussion**

319 The abrupt increase in size of *C. gibba* detected in the stratigraphic records from the Po and  
320 Isonzo prodeltas and the observation that large individuals are invariably rare in the pre-  
321 Anthropocene assemblages at sites with slow sedimentation demonstrate that the shift in  
322 maximum shell size from 5 to 10-15 mm occurred in the whole northern Adriatic Sea (figures  
323 1A, 2A). The comparison of the Holocene with the late 20<sup>th</sup> century assemblages  
324 demonstrates that this change reflects community-wide shift because it was associated with a  
325 shift in genus-level molluscan composition (figure 2B), characterized by an increase in the  
326 dominance of *C. gibba* (figure 2C). Although *C. gibba* was a persistent subset of molluscan  
327 communities during the Holocene (49-50), it became dominant relative to other molluscan  
328 species in the 20<sup>th</sup> century. The bimodality of abundances prior to and after the transition in  
329 the 20<sup>th</sup> century (figure 2C) is a diagnostic attribute of abrupt ecological transitions (51). The  
330 intermediate position of Anthropocene death assemblages with *C. gibba* located between  
331 Holocene assemblages and Anthropocene living assemblages is probably driven by  
332 taphonomic inertia (mixing of Anthropocene shells with older shells of other species).  
333 Multiple lines of evidence indicate that the regime shift was determined by high frequency of  
334 seasonal hypoxia. First, the increase in size and dominance of *C. gibba* coincided with the late  
335 20<sup>th</sup> century eutrophication that was coupled with an increase in the frequency of hypoxic  
336 events (36, 52). Although seasonal hypoxia occasionally affected benthic communities also  
337 prior to the 20<sup>th</sup> century, the recurrence of hypoxic events was less frequent (38). Second,  
338 assemblages that remained small-sized in the 20<sup>th</sup> century were located above the seasonal

339 thermocline at Isonzo prodelta and in the Gulf of Venice, and thus, were not affected by  
340 seasonal hypoxia. Third, both size indices increase with the relative frequency of seasonal  
341 hypoxia at 16 sites (figure 2B), and the abrupt increase in the 95<sup>th</sup> percentile log-length  
342 indicates that the shift between the two states follows a threshold-type dynamic and can  
343 already occur if seasonal hypoxia occurs in one year per decade. *C. gibba* was observed to  
344 grow rapidly to > 11 mm over two years in the aftermath of seasonal anoxia (53). Direct  
345 biological observations showed that seasonal mass mortalities in the Adriatic Sea negatively  
346 affected predators and substrate-destabilizing burrowers, including burrowing shrimps,  
347 echinoids, holothurians, predatory asteroids and muricid gastropods (54), in contrast to  
348 hypoxia-tolerant *C. gibba* (55-56). The recovery of these taxa in the wake of hypoxic events is  
349 delayed and occurs over several years (57), allowing *Corbula* dominance also in years  
350 without seasonal hypoxic events. The size and dominance increase following the shift to  
351 higher frequency might be hypothesized to be driven by the predatory and competitive release  
352 and by high tolerance of *C. gibba* to seasonal hypoxia (58). This release hypothesis is  
353 congruent with the decline in abundance of predatory gastropods observed here and with the  
354 20<sup>th</sup> century decline in the depth of the surface mixed layer declined from several decimeters  
355 documented at Po and Isonzo prodeltas on the basis of higher preservation of flood layers,  
356 reduced mottling, and reduced time averaging (36).

357         Although low sedimentation rates that lead to multi-decadal or millennial time  
358 averaging will strongly reduce temporal variance in body size and will bias abrupt shifts  
359 towards gradual trends, relatively high sedimentation rates (> 0.2 cm/y) are also not sufficient  
360 for the preservation of high-resolution ecological dynamic in the fossil record if associated  
361 with bioturbation. However, the temporal association of the size and compositional changes in  
362 the molluscan community with the declining bioturbation indicates a common cause behind  
363 the regime shift and its preservation potential in the fossil record. We thus posit that the

364 preservation of abrupt regime shifts in the stratigraphic record is triggered by the pervasive  
365 ecosystem change of sufficient, decadal-scale duration that is associated with the decline in  
366 bioturbational mixing, especially in settings with high to moderate net accumulation rates and  
367 without long hiatuses. The Anthropocene regime shifts in the nature of macrobenthic  
368 communities in the northern Adriatic Sea are not only unprecedented relative to the Holocene  
369 history but are also sufficiently strong and temporally persistent so that they have the potential  
370 to be distinctly preserved in the stratigraphic record, paralleling Anthropocene shifts in  
371 geochemical and microbiotic proxies documented in marginal marine environments (59-60).  
372 We suggest that differences in the intensity of bioturbation between extinction regimes with  
373 limited bioturbation and background regimes with intense bioturbation can generate a  
374 dichotomy in the resolution of the marine fossil record on continental shelves. On one hand,  
375 the majority of the fossil record that formed in shelf ecosystems with intense bioturbation  
376 throughout most of the Holocene is probably averaged to centuries or millennia (61) and rich  
377 in gaps (62). On the other hand, the window for preservation of highly-resolved ecological  
378 dynamic on marine shelves probably opens in the aftermath of anthropogenic regime shifts on  
379 the present-day shelves and was probably open in the wake of major ecosystem perturbations  
380 in the past (63). The window for preservation is not equivalent to anoxic conditions that  
381 simply exclude burrowers but is rather determined by the recovery dynamic of burrowers in  
382 the aftermath of disturbances, e.g., by time to habitat recolonization from regions not affected  
383 by extinctions, by incumbency and by source-sink effects at ecological scales, or by time to  
384 speciation at evolutionary time scales.

385

386

### 387 **Data access and availability**

388 Original size data will be uploaded to Data Dryad.

389 **Author contributions:**

390 A.T. and M.Z. designed the research, P.G.A., T.F., I.G., A.H., M.K., R.N., V.N. and D.S.  
391 collected the data, A.T. compiled and analyzed the data, and all authors discussed the results  
392 and contributed to the writing of the manuscript.

393 **Competing interests.** We declare we have no competing interests.

394 **Funding.** This study was funded by the Austrian Science Fund (FWF project P24901), the  
395 Slovak Scientific Grant Agency (VEGA 0169-19), Slovak Research and Development  
396 Agency (APVV17-0555), and the National Science Foundation (EAR-0920075 and EAR-  
397 1559196).

398 **Acknowledgements.** The authors thank S.M. Holland and an anonymous referee for critical  
399 comments.

400 **Electronic Supplementary Material** includes details on data, methods, tables and figures.

401

402 **References**

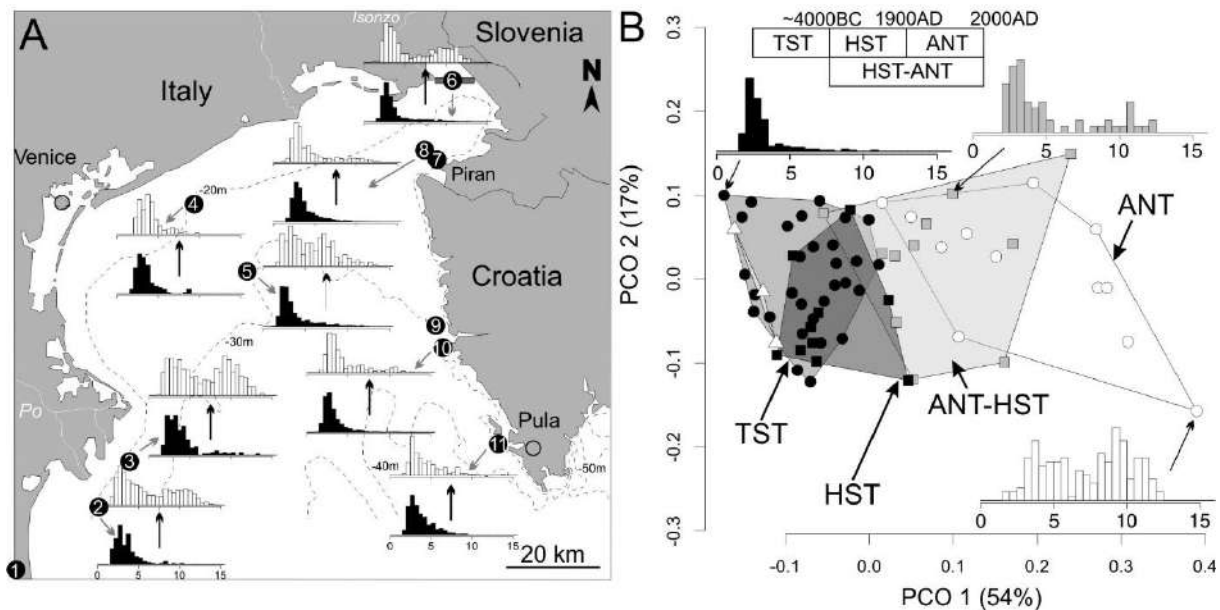
- 403 1. Petersen JK, Hansen JW, Laursen MB, Clausen P, Carstensen J, Conley DJ 2008 Regime  
404 shift in a coastal marine ecosystem. *Ecol Appl* **18**, 497-510.
- 405 3. Villnäs A, Norkko A 2011 Benthic diversity gradients and shifting baselines: implications  
406 for assessing environmental status. *Ecol Appl* **21**, 2172-2186.
- 407 3. Rombouts I et al 2013 Evaluating marine ecosystem health: case studies of indicators using  
408 direct observations and modelling methods. *Ecol Indic* **24**, 353-365.
- 409 4. Di Camillo CG, Cerrano C 2015 Mass mortality events in the NW Adriatic Sea: phase shift  
410 from slow-to fast-growing organisms. *PloS one* **10**, e0126689.
- 411 5. Rocha J et al. 2015 A holistic view of marine regime shifts. *Philos T Roy Soc B* **370**,  
412 20130273.
- 413 6. Dornelas M, Gotelli NJ, Shimadzu H, Moyes F, Magurran AE, McGill BJ 2019 A balance  
414 of winners and losers in the Anthropocene. *Ecol Lett* **22**, 847-854.
- 415 7. Chase JM et al 2019 Species richness change across spatial scales. *Oikos* **128**, 1079-1091.
- 416 8. Aronson RB, Macintyre IG, Wapnick CM, O'Neill MW 2004 Phase shifts, alternative  
417 states, and the unprecedented convergence of two reef systems. *Ecology* **85**, 1876-1891.

- 418 9. Pandolfi JM and Jackson, J.B., 2006. Ecological persistence interrupted in Caribbean coral  
419 reefs. *Ecology Letters* **9**, 818-826.
- 420 10. Kidwell SM 2007. Discordance between living and death assemblages as evidence for  
421 anthropogenic ecological change. *Proc Natl Acad Sci USA* **104**, 17701-17706.
- 422 11. Williams JW, Blois JL, Shuman BN 2011 Extrinsic and intrinsic forcing of abrupt  
423 ecological change: case studies from the late Quaternary. *J Ecol* **99**, 664-677.1.
- 424 12. Tomašových, A. and Kidwell, S.M., 2017. Nineteenth-century collapse of a benthic  
425 marine ecosystem on the open continental shelf. *Proc Biol Sci* **284**, 20170328.
- 426 13. Keller G et al. 2018 Environmental changes during the cretaceous-Paleogene mass  
427 extinction and Paleocene-Eocene thermal maximum: implications for the  
428 Anthropocene. *Gondwana Res* **56**, 69-89.
- 429 14. Aberhan M, Kiessling W 2015 Persistent ecological shifts in marine molluscan  
430 assemblages across the end-Cretaceous mass extinction. *Proc Natl Acad Sci USA* **112**, 7207-  
431 7212.
- 432 15. Penn JL et al. 2018 Temperature-dependent hypoxia explains biogeography and severity  
433 of end-Permian marine mass extinction. *Science* **362**, eaat1327.
- 434 16. Kidwell SM, Tomasovych A 2013 Implications of time-averaged death assemblages for  
435 ecology and conservation biology. *Annu Rev Ecol Evol S* **44**, 539-563.
- 436 17. Kosnik MA et al. 2017 Sediment mixing and stratigraphic disorder revealed by the age-  
437 structure of *Tellina* shells in Great Barrier Reef sediment. *Geology* **35**, 811-814.
- 438 18. Rabalais NN et al. 2007 Sediments tell the history of eutrophication and hypoxia in the  
439 northern Gulf of Mexico. *Ecol Appl* **17**, S129-S143.
- 440 19. Willis KJ et al. 2010 Biodiversity baselines, thresholds and resilience: testing predictions  
441 and assumptions using palaeoecological data. *Trends Ecol Evol* **25**, 583-591.
- 442 20. Jonkers L et al. 2013 Global change drives modern plankton communities away from the  
443 pre-industrial state. *Nature* **570**, 372-375.
- 444 21. Leonard-Pingel JS et al. 2019 Gauging benthic recovery from 20th century pollution on  
445 the southern California continental shelf using bivalves from sediment cores. *Mar Ecol Prog*  
446 *Ser* **615**, 101-119.
- 447 22. Tomašových A, Kidwell SM, Alexander CR, Kaufman DS 2019 Millennial-scale age  
448 offsets within fossil assemblages: result of bioturbation below the taphonomic active zone and  
449 out-of-phase production. *Paleoceanogr Paleocl* **34**, 954-977.
- 450 21. Sadler PM 1981 Sediment accumulation rates and the completeness of stratigraphic  
451 sections. *J Geol* **89**, 569-584.

- 452 22. Tomašových A, Kidwell SM 2010 The effects of temporal resolution on species turnover  
453 and on testing metacommunity models. *Am Nat* **175**, 587-606.
- 454 23. Kemp DB et al. 2015 Maximum rates of climate change are systematically underestimated  
455 in the geological record. *Nature Comm* **6**, 8890.
- 456 24. Holland SM 2016 The non-uniformity of fossil preservation. *Philos T Roy Soc B* **371**,  
457 20150130.
- 458 25. Löwemark L, Grootes PM 2004 Large age differences between planktic foraminifers  
459 caused by abundance variations and *Zoophycos* bioturbation. *Paleoceanography* **19**, PA2001.
- 460 26. Steiner Z, Lazar B, Levi S, Tsroya S, Pelled O, Bookman R, Erez J 2016 The effect of  
461 bioturbation in pelagic sediments: lessons from radioactive tracers and planktonic  
462 foraminifera in the Gulf of Aqaba, Red Sea. *Geochim Cosmochim Ac* **194**, 139-152.
- 463 27. Twitchett RJ 2007 The Lilliput effect in the aftermath of the end-Permian extinction  
464 event. *Palaeogeogr Palaeoclimatol Palaeoecol* **252**, 132-144.
- 465 28. Levin LA, Ekau W, Gooday AJ, Jorissen F, Middelburg JJ, Naqvi SWA, Neira C,  
466 Rabalais NN, Zhang J 2009 Effects of natural and human-induced hypoxia on coastal benthos,  
467 *Biogeosciences* **6**, 2063–2098,
- 468 29. Rick TC, Reeder-Myers LA, Hofman CA, Breitburg D, Lockwood R, Henkes G, Kellogg  
469 L, Lowery D, Luckenbach MW, Mann R, Ogburn MB 2016 Millennial-scale sustainability of  
470 the Chesapeake Bay Native American oyster fishery. *Proc Natl Acad Sci USA* **113**, 6568-  
471 6573.
- 472 30. Payne JL et al. 2016 Ecological selectivity of the emerging mass extinction in the oceans.  
473 *Science* **353**, 1284-1286.
- 474 31. Dornelas M et al. 2013 Quantifying temporal change in biodiversity: challenges and  
475 opportunities. *Proc Biol Sci* **280**, 20121931.
- 476 32. Hunt G. 2012 Measuring rates of phenotypic evolution and the inseparability of tempo  
477 and mode measuring rates of phenotypic evolution. *Paleobiology* **38**, 351-373.
- 478 33. Amorosi A, et al 2003 Facies architecture and latest Pleistocene–Holocene depositional  
479 history of the Po Delta (Comacchio area), Italy. *J Geol* **111**, 39-56.
- 480 34. Scarponi D, Kaufman D, Amorosi A, Kowalewski M 2013 Sequence stratigraphy and the  
481 resolution of the fossil record. *Geology* **41**, 239-242.
- 482 35. Albano PG, Gallmetzer I, Haselmair A, Tomašových A, Stachowitsch M, Zuschin M,  
483 2018 Historical ecology of a biological invasion: the interplay of eutrophication and pollution  
484 determines time lags in establishment and detection. *Biological Invasions* **20**, 1417-1430

- 485 36. Tomašových A et al. 2018 Tracing the effects of eutrophication on molluscan  
486 communities in sediment cores: outbreaks of an opportunistic species coincide with reduced  
487 bioturbation and high frequency of hypoxia in the Adriatic Sea. *Paleobiology* **44**, 575-602.
- 488 37. Tomašových A, et al. 2019 A decline in molluscan carbonate production driven by the  
489 loss of vegetated habitats encoded in the Holocene sedimentary record of the Gulf of  
490 Trieste. *Sedimentology* **66**, 781-807.
- 491 38. Tomašových A et al. 2017 Stratigraphic unmixing reveals repeated hypoxia events over  
492 the past 500 yr in the northern Adriatic Sea. *Geology* **45**, 363-366.
- 493 39. Schnedl SM, et al. 2018 Molluscan benthic communities at Brijuni Islands (northern  
494 Adriatic Sea) shaped by Holocene sea-level rise and recent human eutrophication and  
495 pollution. *Holocene* **28**, 1801-1817.
- 496 40. Gallmetzer I, et al. 2019 Tracing origin and collapse of Holocene benthic baseline  
497 communities in the northern Adriatic. *Palaios* **34**, 121-145.
- 498 41. Gavin DG, Oswald WW, Wahl ER, Williams JW 2003 A statistical approach to  
499 evaluating distance metrics and analog assignments for pollen records. *Quaternary Res* **60**,  
500 356-367.
- 501 42. Simpson, GL 2007 Analogue methods in palaeoecology: using the analogue package. *J*  
502 *Stat Softw* **22**, 1-29.
- 503 43. Goberville E, Beaugrand G, Sautour B, Tréguer P 2011 Evaluation of coastal  
504 perturbations: a new mathematical procedure to detect changes in the reference state of  
505 coastal systems. *Ecol Indic* **11**, 1290-1300.
- 506 44. Tomašových A, Kidwell SM 2011 Accounting for the effects of biological variability and  
507 temporal autocorrelation in assessing the preservation of species abundance. *Paleobiology* **37**,  
508 332-354.
- 509 45. Anderson MJ, Walsh DC 2013 PERMANOVA, ANOSIM, and the Mantel test in the face  
510 of heterogeneous dispersions: what null hypothesis are you testing? *Ecol Monogr* **83**, 557-  
511 574.
- 512 46. Hunt G 2008 Gradual or pulsed evolution: when should punctuational explanations be  
513 preferred? *Paleobiology* **34**, 360-377.
- 514 47. Hunt G, Hopkins MJ, Lidgard, S 2015 Simple versus complex models of trait evolution  
515 and stasis as a response to environmental change. *Proc Natl Acad Sci USA* **112**, 4885-4890.
- 516 48. Sheets HD, Mitchell CE 2001 Why the null matters: statistical tests, random walks and  
517 evolution. In *Microevolution Rate, Pattern, Process* (pp. 105-125). Springer, Dordrecht.

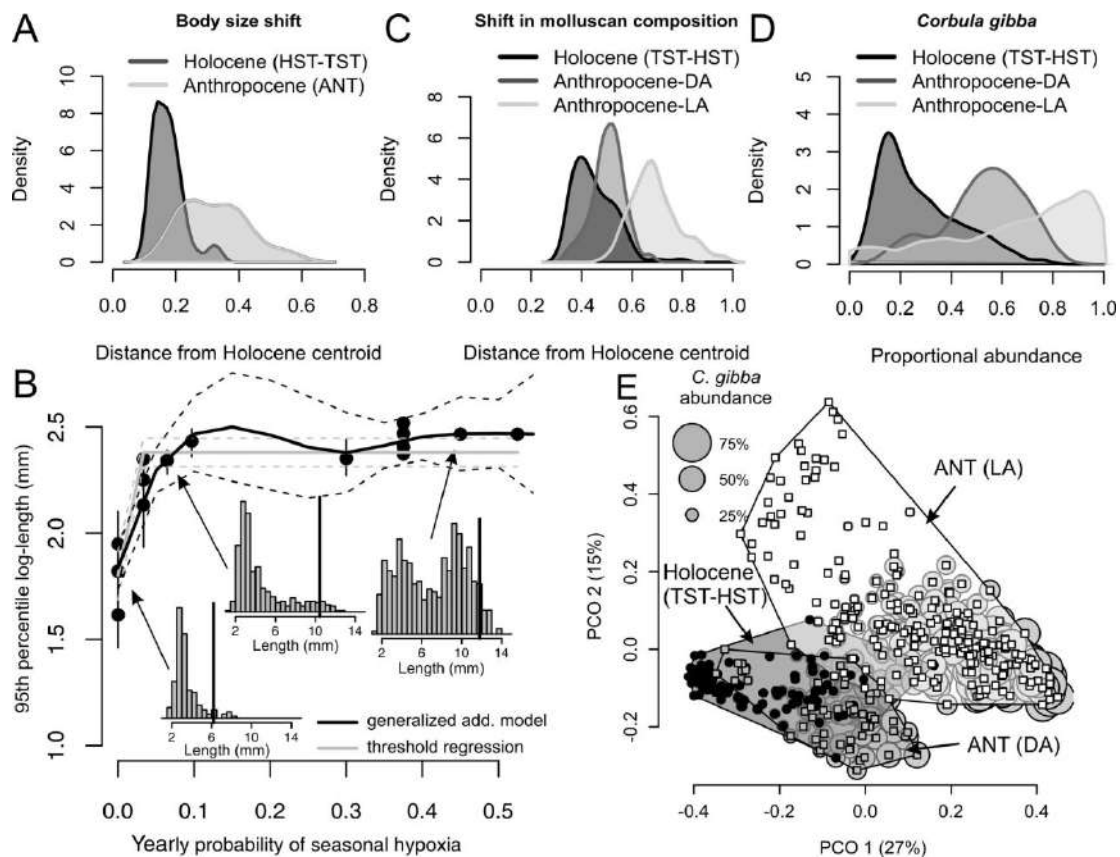
- 518 49. Scarponi D, Kowalewski M 2007 Sequence stratigraphic anatomy of diversity patterns:  
519 Late Quaternary benthic mollusks of the Po Plain, Italy. *Palaios* **22**, 296-305.
- 520 50. Kowalewski M, Wittmer JM, Dexter TA, Amorosi A, Scarponi D 2015 Differential  
521 responses of marine communities to natural and anthropogenic changes. *Proc Biol Sci* **282**,  
522 20142990.
- 523 51. Bestelmeyer BT et al 2011 Analysis of abrupt transitions in ecological  
524 systems. *Ecosphere* **2**, 1-26.
- 525 52. Justić D 1991 Hypoxic conditions in the northern Adriatic Sea: historical development  
526 and ecological significance. *Geol Soc Spec Publ* **58**, 95-105.
- 527 53. Hrs-Brenko M 2003 The role of bivalve *Corbula gibba* (Olivi, 1792) (Corbulidae,  
528 Mollusca Bivalvia) in the recruitment of benthic communities in the northern  
529 Adriatic. *Pomorski Zbornik* **41**, 195–208.
- 530 54. Stachowitsch M 1984 Mass mortality in the Gulf of Trieste: the course of community  
531 destruction. *Mar Ecol* **5**, 243-264.
- 532 55. Holmes SP, Miller N 2006, Aspects of the ecology and population genetics of the bivalve  
533 *Corbula gibba*. *Mar Ecol Prog Ser* **315**, 129-140.
- 534 56. Stachowitsch M 1991 Anoxia in the Northern Adriatic Sea: rapid death, slow recovery.  
535 *Geol Soc Spec Publ* **58**, 119-129.
- 536 57. Riedel B, Pados T, Pretterebner K, Schiemer L, Steckbauer A, Haselmair A, Zuschin M,  
537 Stachowitsch M 2014 Effect of hypoxia and anoxia on invertebrate behaviour: ecological  
538 perspectives from species to community level. *Biogeosciences* **11**, 1491-1518.
- 539 58. Yoder JB et al 2010 Ecological opportunity and the origin of adaptive radiations. *J Evol*  
540 *Biol* **23**, 1581-1596.
- 541 59. Waters CN et al 2016 The Anthropocene is functionally and stratigraphically distinct from  
542 the Holocene. *Science* **351**, aad2622.
- 543 60. Wilkinson IP et al. 2014 Microbiotic signatures of the Anthropocene in marginal marine  
544 and freshwater palaeoenvironments. *Geol Soc Spec Publ* **395**, 185-219.
- 545 61. Kidwell SM 2013 Time-averaging and fidelity of modern death assemblages: building a  
546 taphonomic foundation for conservation palaeobiology. *Palaeontology* **56**, 487-522.
- 547 62. Holland SM, Patzkowsky ME 2015 The stratigraphy of mass extinction. *Palaeontology*  
548 **58**, 903-924.
- 549 63. Hofmann RL et al 2015 Loss of the sedimentary mixed layer as a result of the end-  
550 Permian extinction. *Palaeogeogr Palaeoclimatol Palaeoecol* **428**, 1-11

552 **Figure Legends**

553  
 554 **Figure 1.** Size distributions of *C. gibba* in Holocene (TST and HST) and Anthropocene (20<sup>th</sup>  
 555 century) death assemblages in the northern Adriatic Sea (with the exception of three  
 556 Anthropocene sites from < 10 m depth, all sites are > 10 m deep). A. Holocene-Anthropocene  
 557 site pairs based on eight sites show that right-skewed and thin-tailed HST assemblages (black)  
 558 are replaced by bimodal (under low time averaging) or heavy-tailed (under high averaging)  
 559 Anthropocene assemblages (white). The labels summarize all stations analyzed in this study:  
 560 1 – Po Plain core S10, 2 – Po 4, 3 – Po 3, 4 – Venice, 5 – Station D in the Gulf of Venice, 6 –  
 561 Bay of Panzano transect, 7 – Piran 1, 8 – Piran 2, 9-10 – Rovinj 120 and 38, 11 – Brijuni. The  
 562 shift at sites with high time averaging (sites 5 and 10) is based on shells with (white) and  
 563 without (black) periostracum. B. The size structure of *C. gibba* differs between Holocene  
 564 (TST and HST) and Anthropocene (ANT) assemblages (at sites > 10 m water depth, white  
 565 circles) in principal coordinate analysis based on 10-30 cm-thick increments. The highstand-  
 566 Anthropocene (ANT-HST) assemblages at sites with high time averaging (> 10 m water  
 567 depth) are based on shells with periostracum (gray squares). Three Anthropocene assemblages  
 568 at < 10 m water depth are represented by white triangles.

569

570



571  
 572 **Figure 2.** The size and compositional regime shift between Holocene and Anthropocene  
 573 assemblages and the effect of oxygen concentrations on shell size of *C. gibba*. A. Overlap in  
 574 size structure between Holocene and Anthropocene assemblages: density kernels show that  
 575 the Frechet distances from the Holocene centroid to Anthropocene assemblages (light gray)  
 576 exceed those between Holocene assemblages and the Holocene centroid (dark gray). B. The  
 577 nonlinear increase in the 95<sup>th</sup> percentile log-length of *C. gibba* in death assemblages (based on  
 578 specimens with periostracum only) to the yearly frequency of seasonal hypoxia (based on data  
 579 measured in 1970-2010) can occur if a seasonal hypoxic event occurs at least once during ten  
 580 years. C. Compositional overlap between Holocene and Anthropocene assemblages: density  
 581 kernels show that the Bray-Curtis distances from the Holocene centroid to Anthropocene  
 582 (ANT) living assemblages (LA, light gray) are larger than those among the Holocene  
 583 assemblages (dim gray). Anthropocene death assemblages (DA, dark gray) have intermediate  
 584 position. D. The bimodal distribution of *C. gibba* abundance, with <20% in HST assemblages,  
 585 60% in Anthropocene death assemblages, >80% in living assemblages. E. Genus-level  
 586 compositional separation between Holocene (TST and HST), Anthropocene death  
 587 assemblages, and Anthropocene living assemblages in principal coordinate analysis. The size  
 588 of the bubble plots is scaled to abundance of *C. gibba*.  
 589

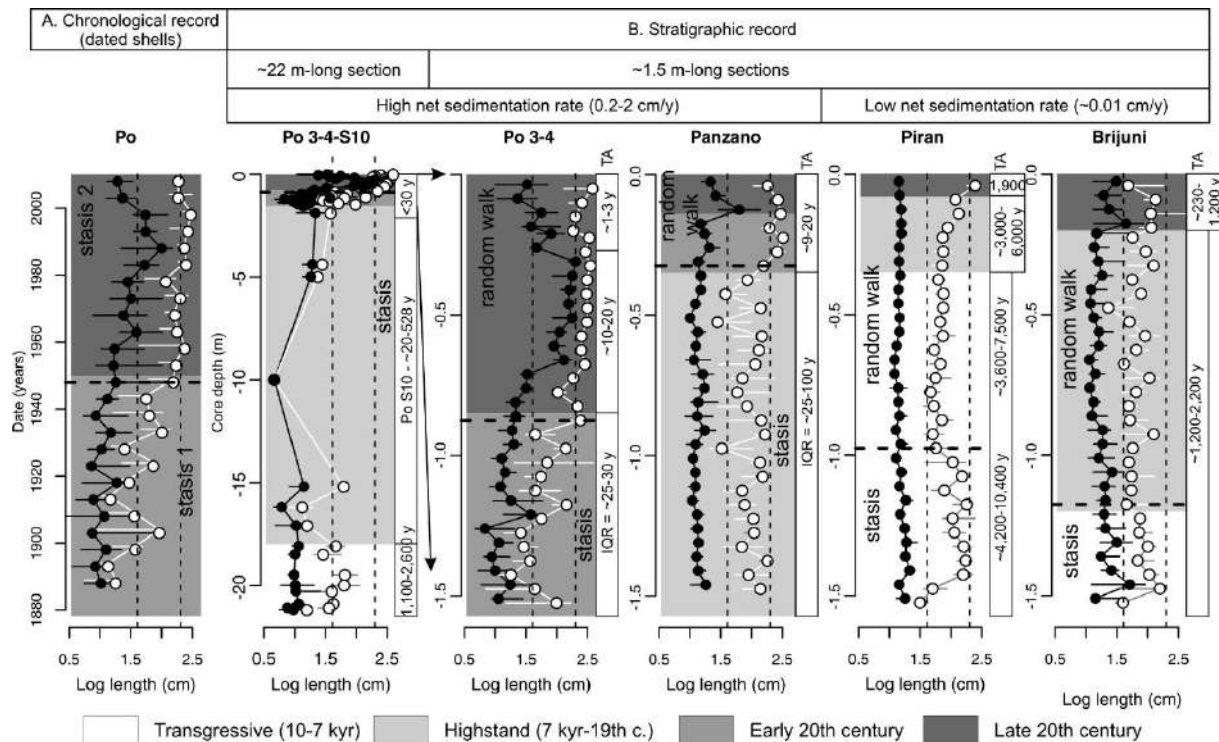
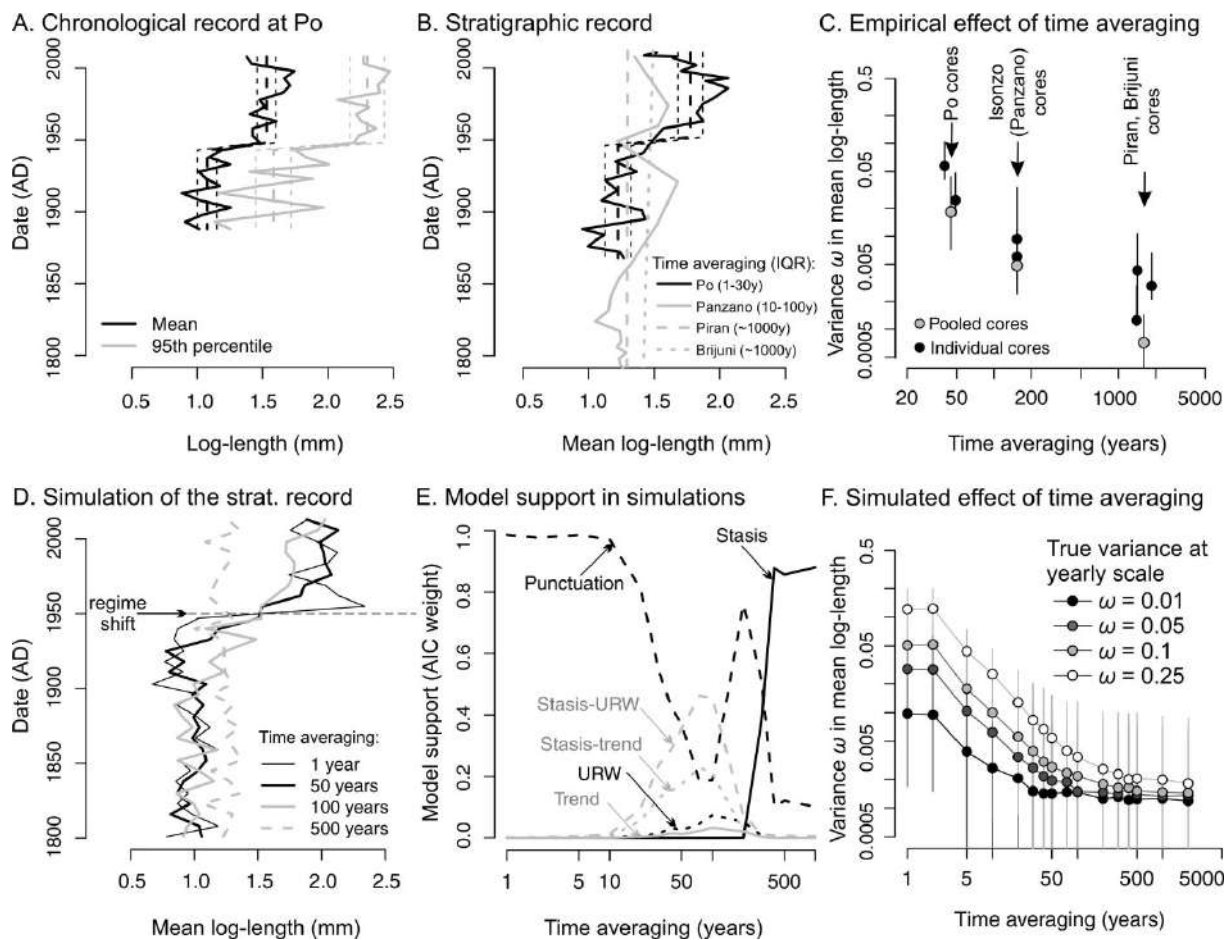


**Figure 3.** Chronological and stratigraphic records in the mean (black points) and the 95<sup>th</sup> percentile log-length (white points) of *Corbula gibba* and the corresponding likelihood models for temporal changes in the 95<sup>th</sup> percentile log-length. The punctuational shift in shell size in the chronological record either translates to stratigraphic punctuation at sites with relatively high sedimentation (at Po and Isonzo with reduced bioturbation) or to strongly muted stratigraphic records at sites with very slow sedimentation (at Piran and Brijuni). The chronological record is based on dated shells partitioned into 5-year cohorts at Po (A). The stratigraphic records are based on 5-10 cm-thick increments at five sites (B). The 1.5 m-long core capturing the last ~150 years (Po 3 and Po 4) is shown separately and together with the S10 core, which extends the record to the onset of the Holocene transgression. Thin vertical dashed lines demarcate the length at 5 and 10 mm. Error bars refer to 95% bootstrapped confidence intervals. Time averaging (TA) refers to the interquartile age range in years.



604

605 **Figure 4.** The sensitivity of size shifts to empirical and simulated time averaging. A. The  
 606 chronological record demonstrates a punctuation in the mean and 95<sup>th</sup> percentile log-length at  
 607 Po in the middle of the 20<sup>th</sup> century. B. The stratigraphic records in the mean log-length at  
 608 four sites differing in time averaging (IQR in brackets). The black dashed line in A-B is the fit  
 609 for the Po prodelta based on the threshold regression. C. The negative relationship between  
 610 time averaging and the variance in mean log-length ( $\omega$ ) observed in the HST increments.  $\omega$   
 611 (with 95% confidence intervals) was estimated at seven sites (two cores at Po, Isonzo, Piran,  
 612 and one core at Brijuni) and in three pooled cores (Po, Isonzo, Piran). D. Stratigraphic records  
 613 of the regime shift in the mean log-length occurring in 1950 AD simulated with four levels of  
 614 time averaging. The thin solid black line refers to one example of non-averaged trajectory (1  
 615 year) and the thick solid black lines refer to time-averaged trajectories. E. Based on D, the  
 616 punctuation is supported at decadal averaging, random-walks and directional trends at 50-200  
 617 years, and stasis at  $> 200$  years. F. The negative relationship between time averaging and  $\omega$   
 618 predicted in Holocene-scale simulations.

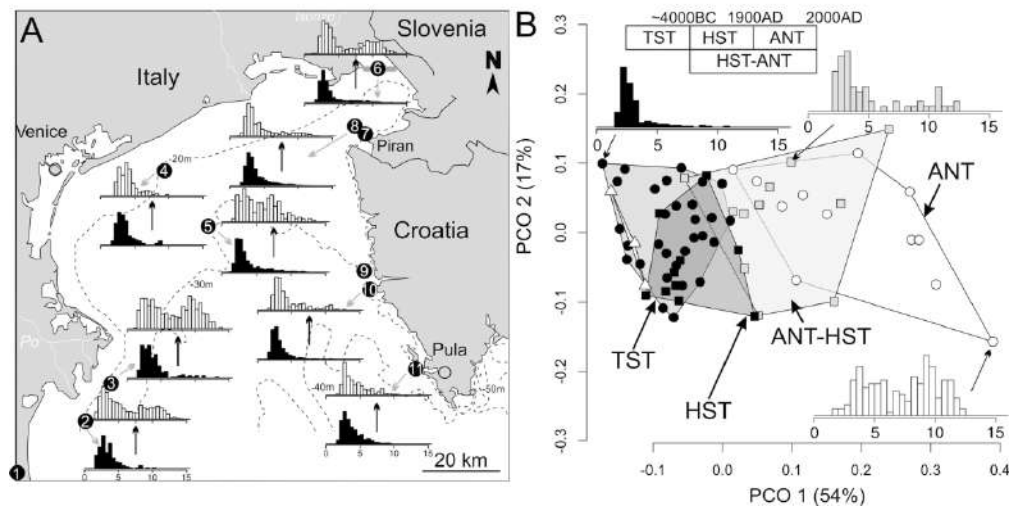


Figure 1. Size distributions of *C. gibba* in Holocene (TST and HST) and Anthropocene (20th century) death assemblages in the northern Adriatic Sea (with the exception of three Anthropocene sites from < 10 m depth, all sites are > 10 m deep). A. Holocene-Anthropocene site pairs based on eight sites show that right-skewed and thin-tailed HST assemblages (black) are replaced by bimodal (under low time averaging) or heavy-tailed (under high averaging) Anthropocene assemblages (white). The labels summarize all stations analyzed in this study: 1 – Po Plain core S10, 2 – Po 4, 3 – Po 3, 4 – Venice, 5 – Station D in the Gulf of Venice, 6 – Bay of Panzano transect, 7 – Piran 1, 8 – Piran 2, 9-10 – Rovinj 120 and 38, 11 – Brijuni. The shift at sites with high time averaging (sites 5 and 10) is based on shells with (white) and without (black) periostracum. B. The size structure of *C. gibba* differs between Holocene (TST and HST) and Anthropocene (ANT) assemblages (at sites > 10 m water depth, white circles) in principal coordinate analysis based on 10-30 cm-thick increments. The highstand-Anthropocene (ANT-HST) assemblages at sites with high time averaging (> 10 m water depth) are based on shells with periostracum (gray squares). Three Anthropocene assemblages at < 10 m water depth are represented by white triangles.

180x97mm (300 x 300 DPI)

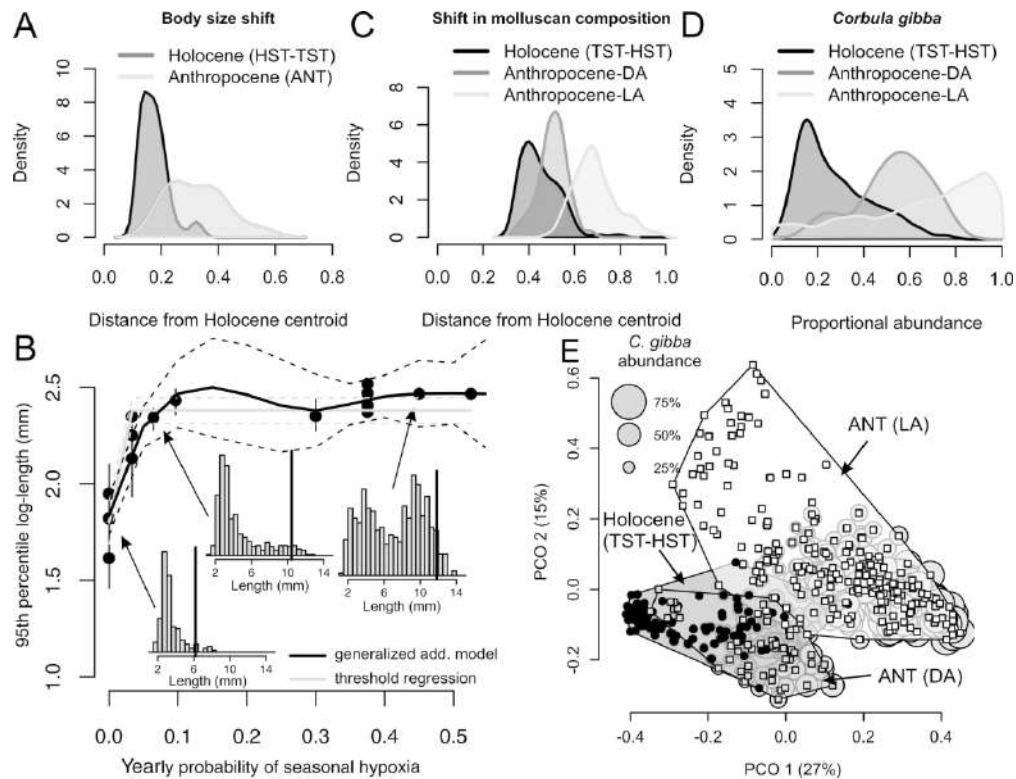


Figure 2. The size and compositional regime shift between Holocene and Anthropocene assemblages and the effect of oxygen concentrations on shell size of *C. gibba*. A. Overlap in size structure between Holocene and Anthropocene assemblages: density kernels show that the Fréchet distances from the Holocene centroid to Anthropocene assemblages (light gray) exceed those between Holocene assemblages and the Holocene centroid (dark gray). B. The nonlinear increase in the 95th percentile log-length of *C. gibba* in death assemblages (based on specimens with periostracum only) to the yearly frequency of seasonal hypoxia (based on data measured in 1970-2010) can occur if a seasonal hypoxic event occurs at least once during ten years. C. Compositional overlap between Holocene and Anthropocene assemblages: density kernels show that the Bray-Curtis distances from the Holocene centroid to Anthropocene (ANT) living assemblages (LA, light gray) are larger than those among the Holocene assemblages (dim gray). Anthropocene death assemblages (DA, dark gray) have intermediate position. D. The bimodal distribution of *C. gibba* abundance, with <20% in HST assemblages, 60% in Anthropocene death assemblages, >80% in living assemblages. E. Genus-level compositional separation between Holocene (TST and HST), Anthropocene death assemblages, and Anthropocene living assemblages in principal coordinate analysis. The size of the bubble plots is scaled to abundance of *C. gibba*.

179x137mm (300 x 300 DPI)

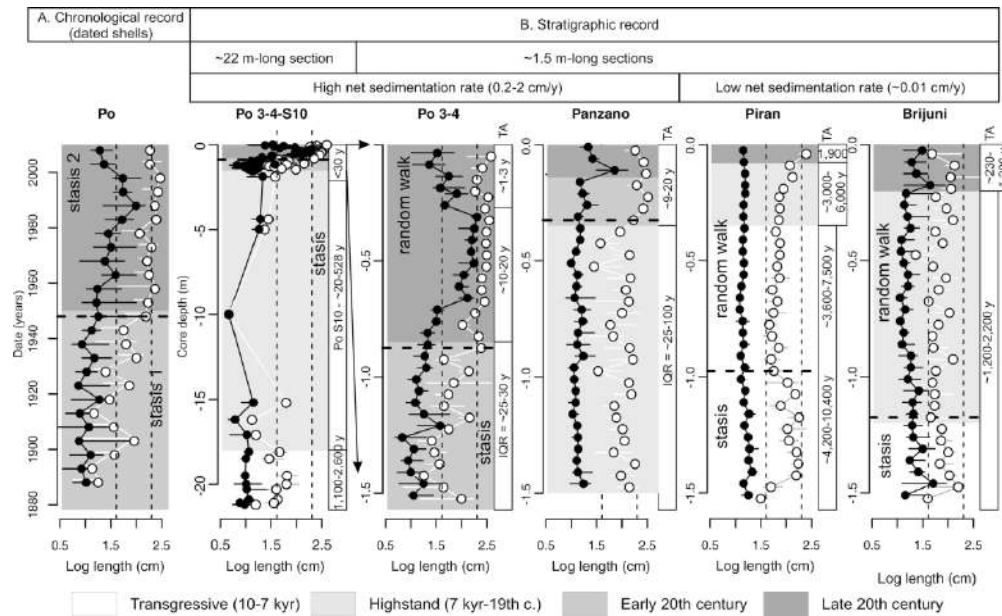


Figure 3. Chronological and stratigraphic records in the mean (black points) and 95th percentile log-length (white points) of *Corbula gibba* and the corresponding likelihood models for temporal changes in the 95th percentile log-length. The punctuational shift in shell size in the chronological record either translates to stratigraphic punctuation at sites with relatively high sedimentation (at Po and Panzano with reduced bioturbation) or to strongly muted stratigraphic records at sites with very slow sedimentation (at Piran and Brijuni). The chronological record is based on dated shells partitioned into 5-year cohorts at Po (A). The stratigraphic records are based on 5-10 cm-thick increments at five sites (B). The 1.5 m-long core capturing the last ~150 years (Po 3 and Po 4) is shown separately and together with the S10 core, which extends the record to the onset of the Holocene transgression. Thin vertical dashed lines demarcate the length at 5 and 10 mm. Error bars refer to 95% bootstrapped confidence intervals. Time averaging (TA) refers to the interquartile age range in years.

201x122mm (300 x 300 DPI)

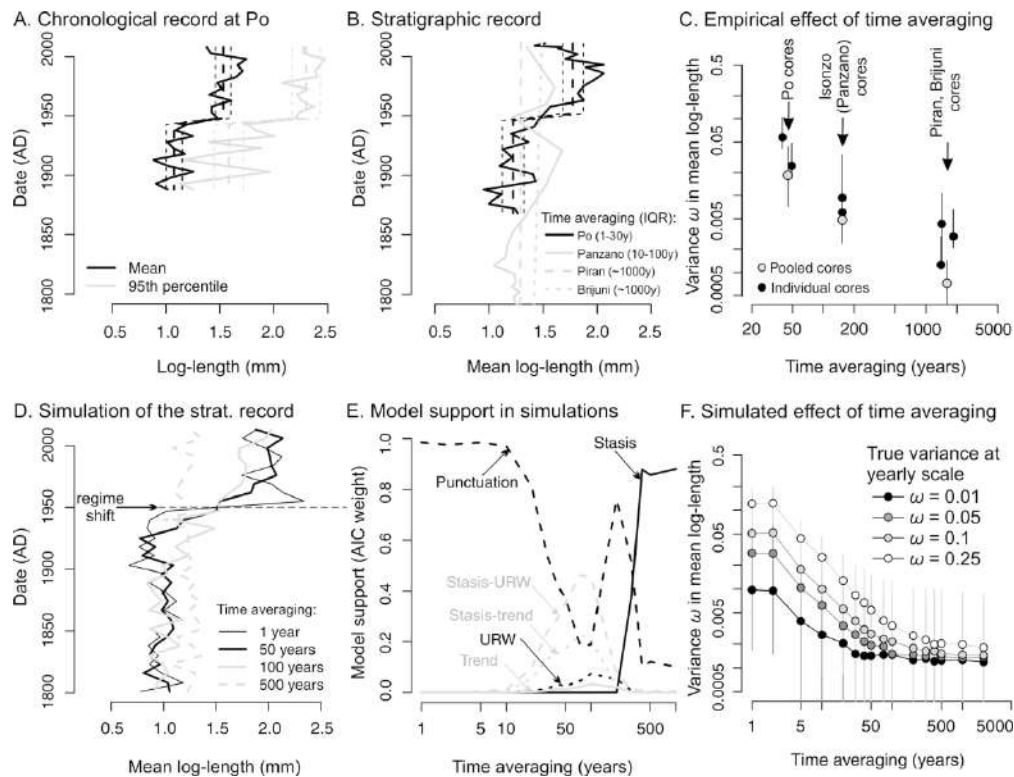


Figure 4. The sensitivity of size shifts to empirical and simulated time averaging. A. The chronological record demonstrates a punctuation in the mean and 95th percentile log-length at Po in the middle of the 20th century. B. The stratigraphic records in the mean log-length at four sites differing in time averaging (IQR in brackets). The black dashed line in A-B is the fit for the Po prodelta based on the threshold regression. C. The negative relationship between time averaging and the variance in mean log-length ( $\omega$ ) observed in the HST increments.  $\omega$  (with 95% confidence intervals) was estimated at seven sites (two cores at Po, Isonzo, Piran, and one core at Brijuni) and in three pooled cores (Po, Isonzo, Piran). D. Stratigraphic records of the regime shift in the mean log-length occurring in 1950 AD simulated with four levels of time averaging. The thin solid black line refers to one example of non-averaged trajectory (1 year) and the thick solid black lines refer to time-averaged trajectories. E. Based on D, the punctuation is supported at decadal averaging, random-walks and directional trends at 50–200 years, and stasis at > 200 years. F. The negative relationship between time averaging and  $\omega$  predicted in Holocene-scale simulations.

179x137mm (300 x 300 DPI)